Monte Carlo simulations of non-Fickian water transport in a saturated porous gel

P. Loureiro de Sousa* and M. Engelsberg
Departamento de Física, Universidade Federal de Pernambuco, 50670-901 Recife-Pernambuco, Brazil
(Received 16 July 1999)

A Monte Carlo algorithm, which incorporates tensile effects as well as diffusion, is proposed. It provides a description of water transport in a drying porous gel close to saturation permitting an interpretation of magnetic resonance imaging profiles. Boltzmann's transformation of the one-dimensional diffusion equation is employed to examine the onset of a non-Fickian transport regime caused by the collective motion of diffusers associated with tensile forces. [S1063-651X(99)11512-5]

PACS number(s): 02.70.Lq, 05.40.−a, 76.70.Fz, 76.60.Pc

I. INTRODUCTION

Water transport in porous systems is a ubiquitous phenomenon present in many important technological applications [1–5] as well as in a variety of natural processes. Among various available experimental techniques, nuclear magnetic resonance (NMR) has been used extensively to probe the nature of the transport processes in various porous systems. At least two different regimes are accessible to NMR. Pulsed-field-gradient (PFG) spin-echo methods can directly yield the self-diffusion coefficient for transport over spatial dimensions which, for large magnetic field-gradient strengths, can be of the order of a few microns. Moreover, in the case of confined diffusion within pores, PFG methods can also yield information about pore microstructure [6–8]. On the other hand, magnetic resonance imaging (MRI) on a macroscopic scale, yields moisture profiles which represent a coarse graining of the transport process over spatial dimensions of the size of an image pixel, typically 0.1 to 1 mm. MRI moisture profiles are useful to monitor water transport in the presence of an external concentration gradient or an applied external pressure or both [1–5]. In some cases such processes can also be described as Fickian diffusion but with a diffusivity which may be different from the self-diffusion constant [3].

Moisture profiles obtained by MRI in cases such as cement drying [1] in a nonsaturated regime or water intake in Nylon 6.6 [3] reveal a Fickian transport processes, albeit with concentration-dependent diffusivities. Under closer scrutiny, even in the case of Nylon 6.6, for large water concentration and temperature not too high above ambient, some evidence of non-Fickian transport is also apparent [3]. On the other hand, in some food products, moisture profiles obtained during drying under special conditions appear not to be at all describable by Fickian diffusion [4,9].

A model food gel (MFG), which simulates the transport properties and texture of some food products, and can also be shaped into convenient geometrical forms, has been proposed. This MFG is composed of agar, water, and microcrystalline cellulose (MCC) in suitable proportions [10]. It forms a porous system which has been studied extensively by various NMR imaging techniques [4,5].

Agar is a biopolymer which, in the sol state, is found in the form of random coils. The gelation process is believed to combine these coils into double helices [11], which aggregate into domains separated by relatively large intercommunicating pores. Water molecules can be either ''free'' or ''bound'' to biopolymer chains and can exchange at rates which appear to be fast compared with NMR transverse relaxation times [11]. Moreover, effectively bound, nonexchanging, water molecules and protons attached to the biopolymer chains do not contribute to MRI intensity. Given their many applications, agar hydrogels have been studied extensively by several methods [11–14]. Of particular interest for the present work is the addition of MCC to an agar hydrogel. This modifies the pore structure yielding a system with peculiar water transport characteristics which simulate the behavior of food products.

In typical experiments, a cylindrical sample of MFG with initial moisture content close to saturation, was allowed to dry laterally and MRI profiles, corresponding to various drying times, were recorded. These profiles, for a given value of drying time, were compared with numerical solutions of Fick's equation at that time with a constant diffusivity acting as an adjustable parameter. A range of values of this parameter was found to be necessary to fit the given profile, suggesting an apparent concentration-dependent diffusivity. Moreover, the range of values of the parameter needed for a fit, was shown to also change considerably for different times. This was interpreted as a signature of non-Fickian transport [4].

Non-Fickian diffusion is considered to be associated with the finite rates at which a structure may change in response to the sorption or desorption of penetrant molecules [15]. This type of diffusion appears to prevail in some glassy systems and polymers. In this paper the onset of a non-Fickian transport regime is examined from a different point of view, which is expected to be relevant in nearly saturated porous systems. Using Monte Carlo simulations we show that if, in addition to random molecular motion, one also includes collective motion of fluid clusters caused by tensile forces, non-Fickian transport results. We demonstrate that, for moisture contents close to saturation, the interplay between random molecular forces and tensile forces can explain the observed drying profiles in a MFG [16]. Furthermore, by employing

*Present address: Groupe de RMN, Laboratoire DCSO, Ecole Polytechnique, 91128 Palaiseau, France.

Boltzmann's transformation of the diffusion equation in our Monte Carlo model, we show how this type of non-Fickian regime is approached via a collective reptationlike motion [17].

II. NON-FICKIAN TRANSPORT ALGORITHM

The presence of Fickian transport, with a diffusivity which may be concentration dependent, can be ascertained experimentally. This requires the determination of profiles for a particular geometry which permit a reasonably good realization of Boltzmann's transformation of the one-dimensional diffusion equation [15]. Defining a variable $\eta = x/2\sqrt{t}$, where x represents the spatial coordinate and t denotes time and provided that the initial and boundary conditions can also be expressed only in terms of η, Fickian profiles corresponding to different times should scale into a universal curve when plotted as a function of η. From this master curve the concentration dependence of the diffusivity can be determined [15]. Although this method has been successfully employed in practice with MRI profiles [3], the required measurements can be rather difficult given the impossibility, in some cases, to satisfy the geometrical constraints over a wide range of moisture content.

As an example, the desorption process in our MFG, and also in other cases where non-Fickian transport prevails, is accompanied by shrinkage. With an initial condition of uniform moisture distribution close to saturation (78% water and 22% solid), the radius of a cylindrical sample is reduced by a relatively small amount, of approximately 10%, when moisture content reaches 69%. However, when shrinkage becomes significant, at the later stages of desorption, an appreciable distortion of cylindrical symmetry usually takes place, turning the comparison between measured profiles and simulated ones, somewhat difficult.

Drying profiles in cylindrical samples of the MFG have been obtained with conventional MRI in a magnetic field of 4.0 T [4] and also with very low magnetic field imaging [5] using the electronic Overhauser effect [18]. In the latter case, a large enhancement of the NMR signal is obtained through irradiation of an electron spin resonance transition of a dissolved free radical, prior to data acquisition in the usual MRI mode [19]. It has been shown recently [5] that Overhauser imaging in very low magnetic fields may furnish moisture profiles which are extremely sensitive to small variations of local water content.

Figure 1 shows a moisture profile obtained by Overhauser imaging in a magnetic field of only 16 mT in a cylindrical sample of the MFG. Starting from a largely saturated system with an initially uniform moisture distribution a sample of diameter $2a = 21.4$ mm and 50 mm in height, was exposed to the ambient and allowed to dry laterally in still air. The drying time for the measured profile was 197 min. Also shown in Fig. 1 are numerical solutions of the diffusion equation as a function of r/a for cylindrical symmetry and various values of the diffusion constant. The simulated profiles correspond to $t = 197$ min and a uniform initial moisture distribution $m_w(r,0)$. Here, as in other simulations, we have assumed a boundary condition of constant surface concentration at $r = a$ of negligible value. Since we are dealing only with the initial stages of drying of a largely saturated system

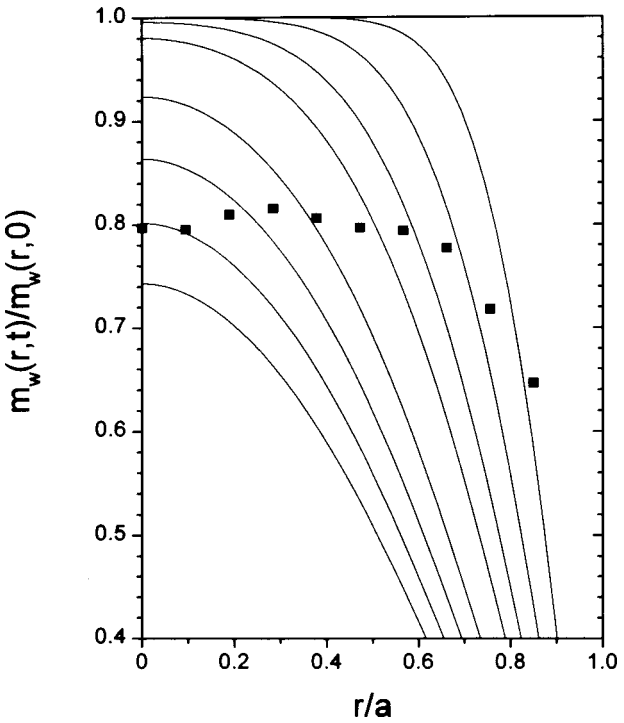

FIG. 1. (—) Moisture profiles obtained from a numerical solution of the diffusion equation in a cylinder of radius $a = 10.7$ mm at $t = 196$ min assuming a constant diffusivity D as a parameter. The diffusivity increases from top to bottom through the following range of values: $D(10^{-5}\,\mathrm{cm^2\,sec^{-1}}) = 0.16$, 0.28, 0.44, 0.59, 084, 1.03, 1.21, and 1.38. $m_w(r,0)$ denotes the initial water distribution assumed to be uniform. (■) Experimental profile in a MFG after a drying time of $t = 196$ min. The initial condition corresponds to a uniform moisture distribution close to saturation. Moisture profiles were determined by Overhauser magnetic resonance imaging.

this simplifying assumption should not greatly affect the results.

While the calculated Fickian profiles of Fig. 1 exhibit a paraboliclike shape, the measured profile in the MFG displays a relatively flat plateau. For longer times, the height of the plateaus decrease with comparatively small changes in shape. This behavior has also been observed in the drying of actual food product such as apples [9] which actually display a texture and porosity resembling our MFG.

From simulated profiles such as those shown in Fig. 1, Schrader *et al.* [4] attempted to determine a concentration dependence of the diffusion constant. They verified that, the apparent diffusivity obtained from this analysis displayed not only a concentration-dependence but also time-dependence, concluding that the transport process was non-Fickian.

It has been proposed [16] that the somewhat puzzling profiles observed in our MFG may be a consequence of the interplay between two effects. One is diffusion, broadly understood as transport of matter resulting from random molecular motion. The other is the effect of tensile forces tending to preserve the integrity of clusters of fluid which form within the random network of capillaries. A familiar phenomenon, which underlines the importance of tensile forces, is the ascending transport of sap through the xylem of trees and plants. The height reached by the water column without breakage, from the roots to the leaves, may by far exceed the maximum height achievable by pulling the water column

with a vacuum pump. To explain this phenomenon [20] one must assume that, under the surface of the leaves, water molecules evaporate one at a time and are individually replaced by molecules pulled from below by surface-tension forces, preserving, in this way, the continuity of the column.

An experiment which clearly demonstrated for the first time the importance of tensile effects in water as it evaporates from the surface of a saturated porous clay vessel was performed by Böhm in Ref. [20]. The interplay between diffusion and tensile forces has been also found to be important for a description of other transport phenomena in porous systems [21] and has been explored extensively by computer simulations using concepts related to invasive percolation [22].

The Monte Carlo method, which we employ in order to incorporate tensile effects, permits, not only a description of MRI moisture profiles in the MFG, but also visualizing the onset of non-Fickian transport in a saturated system. The proposed algorithm for simulating MRI profiles in the MFG involves a two-dimensional square lattice with an inscribed circular boundary of constant radius which simulates a long cylindrical sample. The relatively small shrinkage of the initial stages of desorption is ignored. Each lattice site may be thought to represent a pore and fluid is allowed to diffuse to neighboring pores along capillaries represented by the ''bonds'' between the given site and its nearest neighbors. Diffusers occupying sites linked by nearest neighbors bonds define a cluster.

Given the spatial resolution of available MRI profiles, a square lattice consisting of 40×40 sites was found to be adequate for our simulations. The cylindrical symmetry is simulated by a circular region enclosed within the square lattice. The $N=1600$ sites forming the lattice are initially randomly filled with M diffusers and one of the sites, within the inscribed circle, is randomly chosen as well as one of its nearest neighbors. We first consider purely diffusive transport. In this case, if the chosen lattice site is occupied by a diffuser and the chosen neighbor is empty, the diffuser will jump to the empty site independently of the occupation of other sites. If the chosen lattice site is empty or the chosen neighbor is occupied, a new random choice is performed. Moreover, if a jump occurs, the position of the diffuser is actualized and a new draw is made. Thus, after the process has been repeated N times, each diffuser has attempted on the average one jump and Monte Carlo time is incremented by one unit.

For each ''pixel'' in a simulated profile, the average occupation number of a site over a large number n_r of repetitions is calculated at a given Monte Carlo time. This average occupation number is proportional to the concentration of fluid $m_w(r,t)$ at a given distance and time. External drying conditions are simulated in the algorithm by introducing a probability p_s for a diffuser to be removed from the lattice when it reaches the boundary at $r=a$.

As a check, profiles obtained with a number of repetitions varying between $n_r=4\times 10^5$ and $n_r=10^7$ (for the case of very small values of M/N), were compared with a numerical solution of the diffusion equation for a cylinder of radius a and constant diffusivity D [15]. An evaporation probability $p_s=1$ was assumed in the Monte Carlo simulation and a constant concentration of negligible value at $r=a$ was assumed in the diffusion equation. Denoting by N_{MC} the number of Monte Carlo steps, the ratio N_{MC}/N in the simulation should correspond to the actual adimensional time Dt/a^2, in the numerical solution. Starting in both cases with an initially uniform distribution at $t=0$, excellent agreement between Monte Carlo and numerical profiles was obtained [16], as expected for Fickian diffusion.

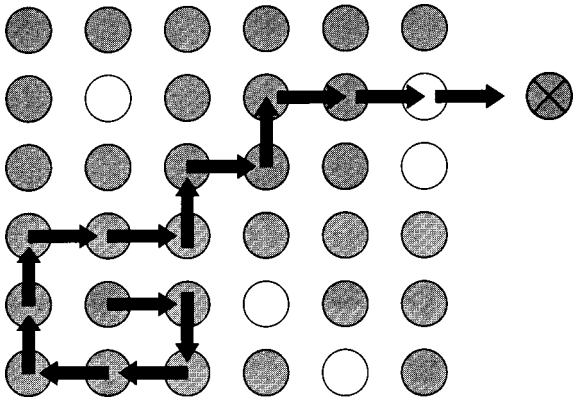

FIG. 2. Schematic representation of the tensile transport algorithm. A surface diffuser ($\times$) evaporates leaving a vacancy which is filled by another diffuser. The process is iterated causing a collective motion of a cluster.

In order to deal with the peculiar profiles observed in our MFG, tensile effects were taken into account by the following modification of the above transport algorithm. After one site and a nearest neighbor have been randomly chosen among N lattice sites, and assuming the first to be occupied and the second empty, the diffuser will jump to the empty site but now its motion may affect the position of other diffusers belonging to the same cluster. For relatively high concentration of diffusers, each site left vacant by the motion of a member of the cluster is filled by another nearest neighbor diffuser, thus preserving the integrity of the aggregates. When several diffusers may jump into the same site, a random choice with equal probability is employed to avoid conflict. Moreover, Monte Carlo time is advanced one unit after N random choices, just as in the case of purely diffusive transport.

As before, a diffuser reaching a site at the boundary may be removed with probability p_s. However, if it evaporates, the vacancy will be filled by a randomly chosen nearest neighbor diffuser. This process is iterated until the vacancy created either reaches a dead end or all its nearest neighbors have already participated in the collective motion. Similarly, when a diffuser belonging to a cluster jumps to an empty site in the bulk, the same collective motion from randomly chosen sites to the site left vacant is performed. Figure 2 shows schematically some of the details of the algorithm.

In addition of provoking a collective reptationlike motion, tensile forces have a different effect. Also the probability of a diffusive jump from a given occupied site to an empty site, must be assumed to depend upon the occupation of other neighboring sites. If an occupied site with an empty neighbor is surrounded, for example, by three filled sites, the diffuser should be assumed to be tightly bound and a relatively low jump probability denoted by $p(3)$ should be assigned. On the contrary, if the occupied site is surrounded by four empty

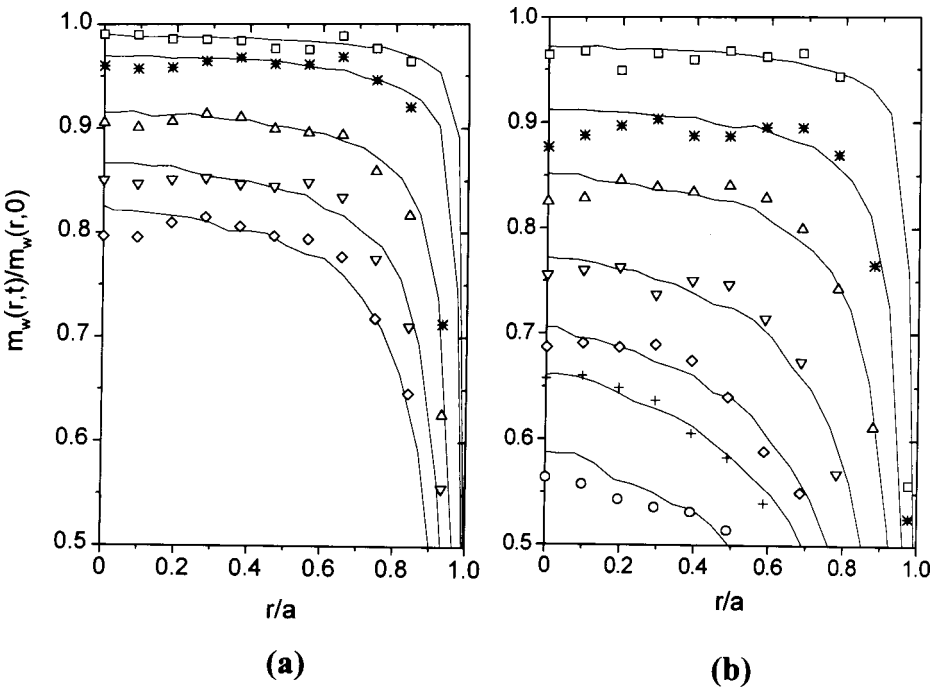

FIG. 3. (a) Measured moisture profiles in a MFG obtained by Overhauser imaging for the following drying times: (□) $t=2$ min, (*) $t=15$ min, (△) $t=76$ min, (▽) $t=98$ min, (◇) $t=176$ min. The full lines are simulated profiles for the following corresponding numbers Monte Carlo steps $N_{MC}=7$, 16, 42, 57, and 114. (b) Measured moisture profiles in a different drying run involving longer times (□) $t=32$ min, (*) $t=53$ min, (△) $t=95$ min, (▽) $t=197$ min, (◇) $t=301$ min, (+) $t=342$ min, and (○) $t=449$ min. The full lines are simulated profiles for the following corresponding numbers of Monte Carlo steps $N_{MC}=15$, 44, 73, 138, 194, 230, and 300.

sites, the corresponding probability is $p(0)$ should be a maximum. Thus, the purely diffusive component of the non-Fickian transport should display a concentration-dependent diffusivity which increases for lower concentrations. The opposite could be concluded from Fig. 1, where higher apparent diffusivities are seen to be needed for a fit of the central part of the profiles where the concentration is higher. Since the transport is non-Fickian this conclusion, drawn from Fig. 1, is not really warranted.

Unlike Fickian diffusion, the profiles in our transport model depend upon the initial concentration of diffusers M/N, representing the degree of saturation of the pores, which is one of the adjustable parameters of the model. The other adjustable parameters are the probabilities $p(z)$, where z denotes the number of occupied nearest neighbors. Taking $p(0)=1$, we have assumed for simplicity $p(1)=p(0)$ and $p(3)=p(2)=\lambda$. Although more realistic choices could be employed, this particular one has the advantage of keeping the number of adjustable parameters to a minimum and still exhibiting the effect of tensile forces upon jump probabilities. Figure 3 shows simulated profiles for various Monte Carlo times with $\lambda=0.2$ and a value of $M/N=0.98$ which appear to be in good agreement with the experimental data. The choice of the parameter M/N affects mainly the shape of the plateaus and its value suggests that only a small fraction of pores are initially empty. The parameter λ, on the other hand, has a more pronounced effect upon the time evolution of the transport process and upon the rate of mass loss. If, for example, a value of λ closer to one were chosen, the number of Monte Carlo steps needed for a given mass loss as the system dries would progressively become larger than observed experimentally.

It is quite instructive to examine more closely the relationship between Monte Carlo time and physical time. Figure 4 shows a plot of Monte Carlo time N_{MC} as a function of real time respectively for simulated and experimental profiles of Fig. 3. For Fickian diffusion with a constant diffusivity D, one expects a ratio $N_{MC}/t=ND/a^2$. Moreover, the value of this ratio obtained from the slope of the straight line of Fig. 4 for our model yields a value $N_{MC}a^2/Nt=0.62\times10^{-5}$ cm^2/sec, which could likewise be interpreted as an effective global diffusivity. In spite of the non-Fickian character of water transport in this MFG suggested by the NMR imaging profiles, global diffusivity values determined for example from desorption measurements are often quoted [10]. Desorption measurements performed in our MFG sample yielded, from a best fit of the mass loss curve to a theoretical, constant diffusivity curve [15], a value 0.57×10^{-5} cm^2/sec. The reasonable agreement between the global diffusivity obtained from a Monte Carlo fit and the experimental value obtained from desorption measurements, in spite of the non-Fickian character of the transport, emphasizes the dominant role of diffusion in determining the rate of mass loss. The collective motion caused by tensile forces, which will be shown to cause non-Fickian behavior, appears to be mainly responsible for a spatial redistribution of fluid.

Although the tensile transport algorithm described above appears to adequately describe the initial stages of desorption in a saturated porous system, an important aspect, has not yet been considered. The texture of the porous system, determined by the size distribution of capillaries and pores, is expected to play an important role. Within the framework of the present model, the collective motion of diffusers assumed in the algorithm should be viewed as a flow, which could

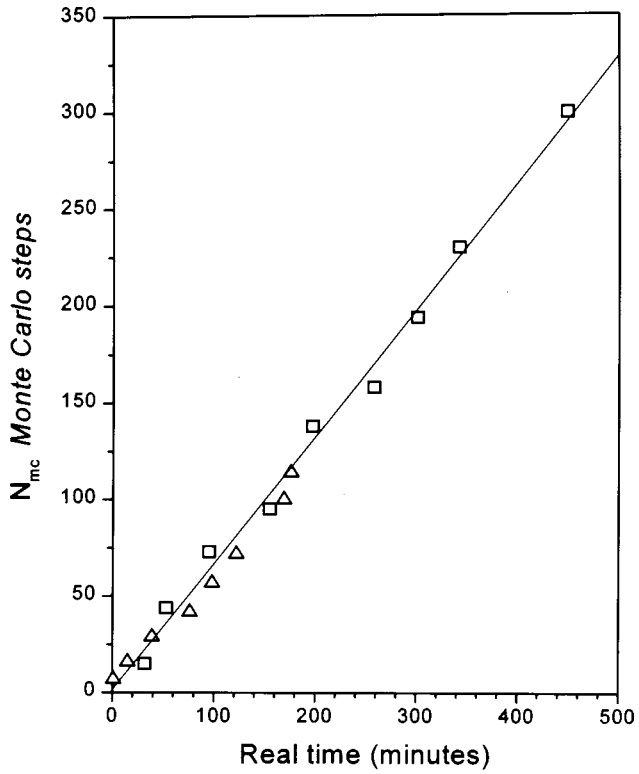

FIG. 4. Number of Monte Carlo steps N_{MC} as a function of real drying times, respectively, for simulated and experimental profiles shown in Fig. 3(a). Obtained from profiles of Fig. 3(a) (△). Obtained from profiles of Fig. 3(b) (□).

only be maintained continuously within a given capillary if its diameter is larger than a critical value. For a given rate of surface evaporation, the tensile strength of water and its viscosity determine the critical diameter of a capillary with given length [20].

Although a detailed description of the distribution of capillaries and of critical diameters is an inherently complex problem, some aspects can be incorporated in a simple way into our model by allowing a finite breakage probability within a moving cluster. Moreover, this breakage probability is expected to be larger for diffusers which are less strongly bound, leading eventually to Fickian transport for concentrations far from saturation.

For example, if one assumes a breakage probability $\Gamma(z)$ which is only significant for diffusers with only one occupied nearest neighbor $(z=1)$, any value $\Gamma(1)\leqslant 0.1$ may be introduced into the algorithm without affecting appreciably the simulated profiles of Fig. 3 However, the effect of adopting, for example $\Gamma(1)=0.1$, is quite significant at low values of M/N, where it leads to a Fickian regime [16].

III. BOLTZMANN'S TRANSFORMATION

One should next consider a more stringent test for non-Fickian behavior and examine which aspects of the above transport algorithm are conducive to the onset of this regime. Fickian diffusion in an isotropic medium is described by the well-known partial differential equation:

$$\partial C/\partial t = \mathrm{div}(D\ \mathrm{grad}\, C), \tag{1}$$

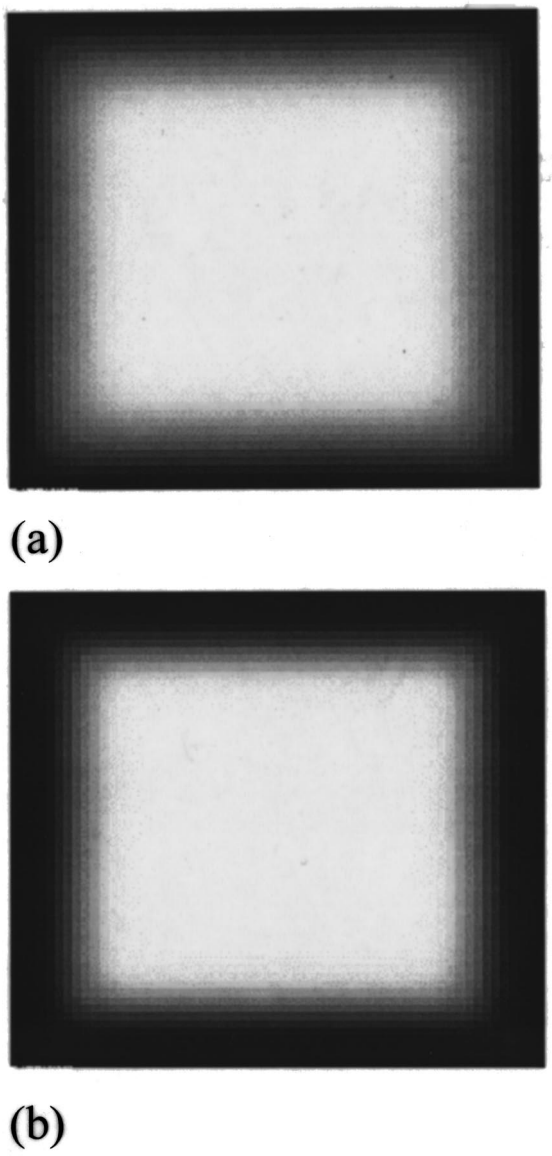

FIG. 5. (a) Simulated MR image of water uptake into an initially empty square lattice with a constant boundary concentration $C(0)=1$, corresponding to saturation. A constant diffusivity Fickian process has been assumed with $N_{MC}=100$. (b) Simulated MR image of water uptake into an initially empty square lattice for the transport mechanism that includes collective motion caused by tensile forces. A value $\lambda=0.2$ has been assumed with a breakage probability $\Gamma(1)=0.1$.

where the concentration of diffusers is denoted by $C(\vec{\mathbf{r}},t)$. Provided the boundary conditions are independent of time, Fickian diffusion takes place if the diffusivity D is either a constant or a function of concentration only.

In one dimension, a knowledge of $C(x,t)$ permits, by a simple transformation due to Boltzmann [15], to determine whether the transport process is Fickian and, this being the case, to also determine the concentration dependence $D(C)$ of the diffusivity. If a new variable $\eta = x/2\sqrt{t}$ is defined, the one-dimensional form of Eq. (1) can be written as

$$-2\eta \frac{dC}{d\eta} = \frac{d}{d\eta}\left(D\frac{dC}{d\eta}\right). \tag{2}$$

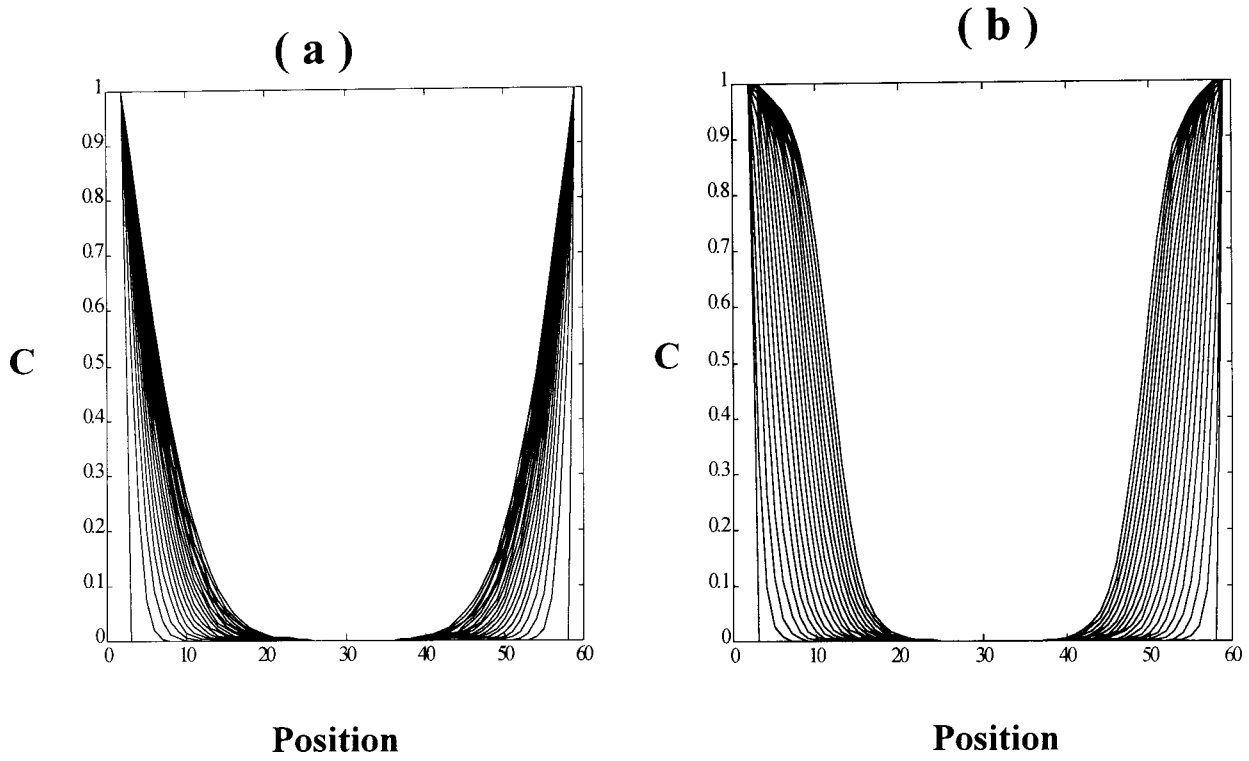

FIG. 6. (a) Simulated profiles for the purely diffusive case obtained through a center line of Fig. 5(a). The number of Monte Carlo steps ranges from $N_{MC}=1$ to $N_{MC}=100$ in increments of five. (b) Simulated profiles for tensile transport, obtained through a center line of Fig. 5(b). The number of Monte Carlo steps ranges from $N_{MC}=1$ to $N_{MC}=100$ in increments of five.

Equation (2) suggests that if the diffusivity $D(C)$ is a function of C only, the concentration $C(\eta)$ should be dependent upon the single variable η, provided the initial and boundary conditions can also be expressed in terms of η alone. A semi-infinite medium [11] with $C=C(0)$ for $x=0$, $t>0$ and $C=0$ for $x>0$, $t=0$, satisfies these requirements. The initial and boundary conditions can be written in this case as

$$C=0 \quad \text{for} \quad \eta\rightarrow\infty \tag{3a}$$

$$C=C(0) \quad \text{for} \quad \eta=0 \tag{3b}$$

which together with Eq. (2) lead to a universal curve $C(\eta)$ provided D is only a function of concentration. The existence of such a master curve for the above geometry, is a signature of Fickian diffusion. Moreover an integration of Eq. (2) yields

$$D(C)=-2\left(\frac{d\eta}{dC}\right)\int_0^C \eta(C')dC'. \tag{4}$$

Thus a knowledge of the master curve and its inverse $\eta(C)$ permits, from Eq. (4), a determination of the concentration dependence of the diffusivity.

In order to study in more detail the onset of non-Fickian behavior in a saturated system in the presence of tensile forces as well as diffusion, our Monte Carlo algorithm was adapted to a geometry where the validity of Boltzmann's transformation could be ascertained. To that end, a condition of water intake into an initially empty lattice, from a boundary, with constant surface concentration $C(0)=1$ corresponding to all surface lattice sites occupied, was adopted. This is analogous to an arrangement that has been actually employed in practice [3], whereby a long square prism of material is immersed in a water bath, while moisture profiles obtained by MRI are recorded at various stages of the intake process.

Figures 5(a) and 5(b) show two simulated images of transverse slices of a square prism immersed in water, with the darker gray scale indicating higher water concentration. Both simulated images in Fig. 5 correspond to the same number $N_{MC}=100$ of Monte Carlo steps, a square lattice of 40×40 sites and 5000 averages. In Fig. 5(a) a condition of Fickian diffusion with constant diffusivity has been assumed. On the other hand, in the simulated image of Fig. 5(b), tensile transport with the same value $\lambda=0.2$ employed in Figs. 3 and a small breakage probability $\Gamma(1)=0.1$ was adopted. It is apparent that, unlike the Fickian case depicted in Fig. 5(a) where water intake progresses gradually, a wet front seems to be propagating in Fig. 5(b). This is more evident in Figs. 6(a) and 6(b), where profiles through the center lines of Figs. 5(a) and 5(b), respectively, are shown. These profiles, which correspond to a number of Monte Carlo steps ranging from $N_{MC}=1$ to $N_{MC}=100$ in increments of five in both cases, show that the conditions for the applicability of Boltzmann's transformation are met for the time interval considered. Since the overlap of the profiles corresponding to water intake from opposite surfaces appears to be very small, a semi-infinite boundary can be safely assumed.

As expected for Fickian diffusion, the profiles of Fig. 6(a) can be scaled into a master curve. If each value of $C(x,t)$ is plotted against an abscissa η, where the position is divided by a quantity proportional to the square root of Monte Carlo

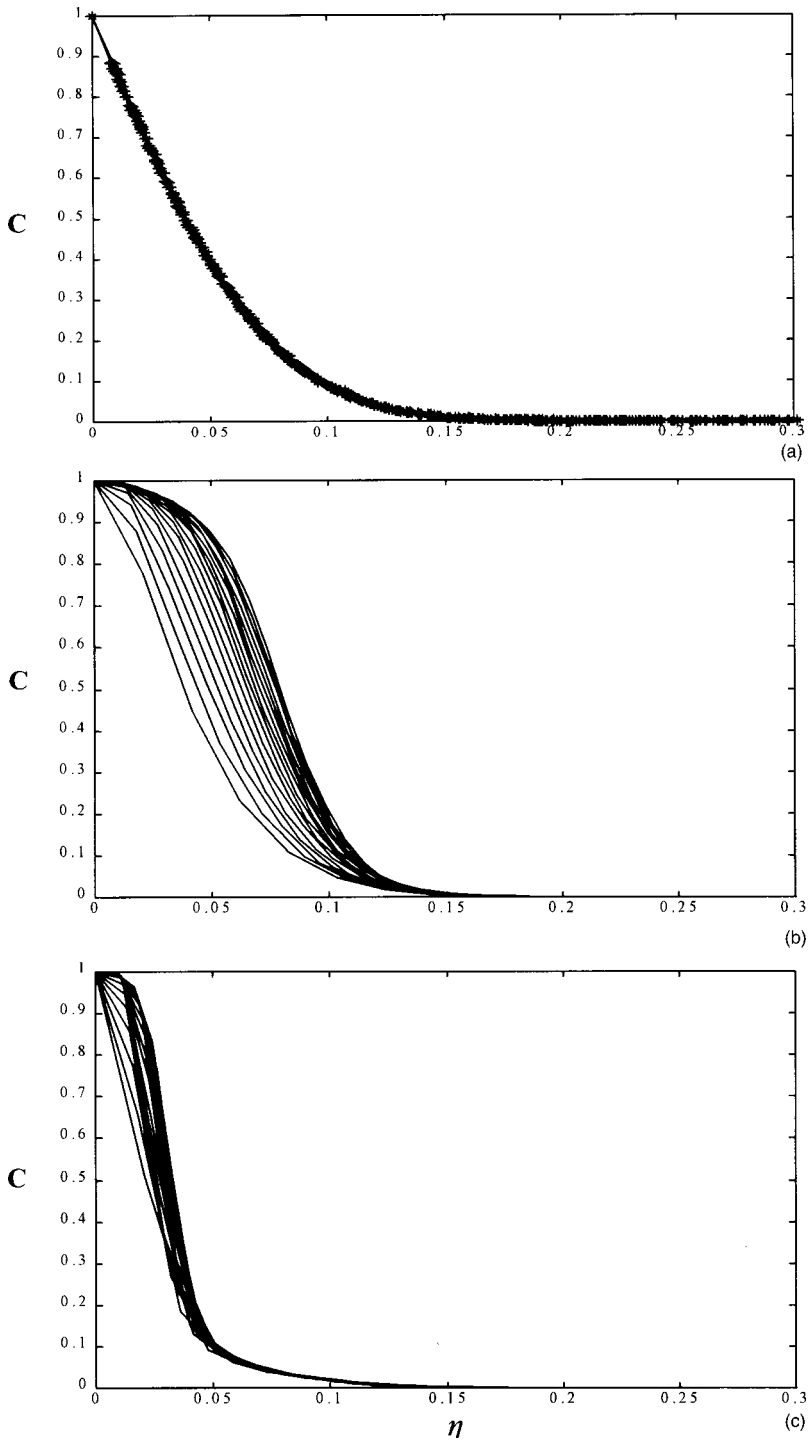

FIG. 7. (a)(●) Master curve for the purely diffusive case obtained from the simulated profiles of Fig. 6(a) using the scaling $\eta \propto x/\sqrt{N_{\mathrm{MC}}}$ of Boltzmann's transformation. The distance x is measured from one of the edges to points in the corresponding family of profiles. (—) Theoretical master curve obtained from an exact numerical solution. (b) Scaling of profiles of Fig. 6(b) according to Boltzmann's transformation. A universal curve is not obtained for the tensile transport model with $\lambda = 0.2$ and $\Gamma(1) = 0.1$, except for very small concentrations. (c) Scaling of profiles obtained for the tensile transport model with $\lambda = 0.2$ and a large breakage probability defined by: $\Gamma(1) = 1$. The Fickian regime appears to be approached at considerable higher concentration than in (b).

time, one obtains the universal curve shown in Fig. 7(a). A comparison between this curve and an exact solution of the diffusion equation for this simple geometry shows excellent agreement.

In contrast, for a tensile transport algorithm, Fig. 7(b) shows that such a scaling is not possible except for very small values of C. The more stringent test provided by Boltzmann's transformation therefore indicates that the Fickian character of the transport process is actually destroyed by the collective reptationlike motion. Furthermore, as the breakage probability is increased, the Fickian regime is approached at higher values of concentration, as expected. This is shown in Fig. 7(c), where a breakage probability $\Gamma(1) = 1$ with $\Gamma(2) = \Gamma(3) = 0$, has been assumed.

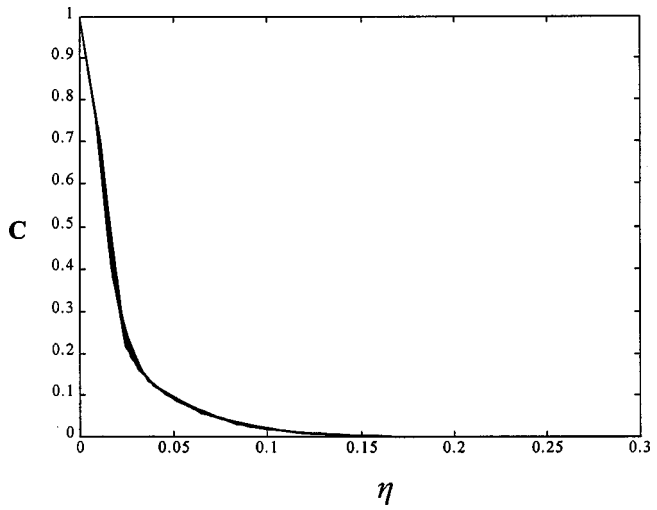

FIG. 8. Master curve obtained by Boltzmann's scaling of several simulated profiles with $\lambda = 0.2$ and a breakage probability $\Gamma(z) = 1$ for all values of z. The suppression of the collective motion leads to a Fickian process with a concentration-dependent diffusivity.

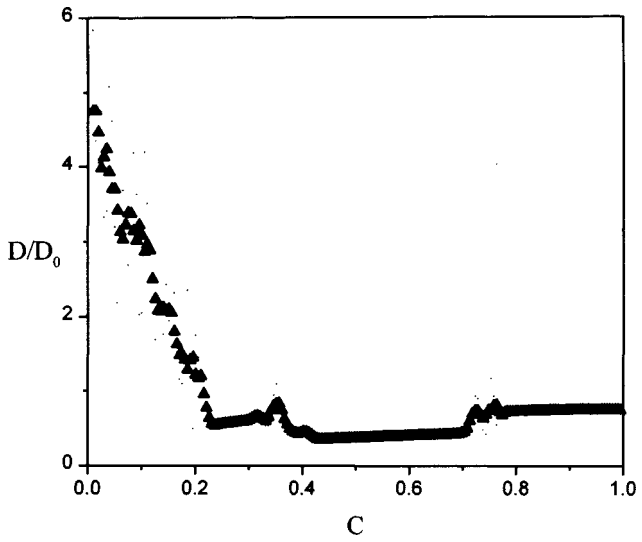

FIG. 9. Concentration dependence of the diffusivity for the Fickian process resulting from making $\lambda = 0.2$ and $\Gamma(z) = 1$. Obtained from the master curve of Fig. 8.

In addition to a collective motion of diffusers, our algorithm also postulates that jump probabilities depend upon the number of nearest neighbors of a given diffuser. The possibility of a modification of the Fickian nature of the transport caused this assumption should also be examined. Figure 8 shows that a universal curve is still obtained when the breakage probability for all clusters $\Gamma(z)$ is made equal to 1, therefore suppressing the collective motion, but a value $\lambda = 0.2$ is still maintained as in Fig. 3. Although the shape of this master curve is quite different from that of Fig. 7(a), the existence of a universal curve confirms that the Fickian nature of the process is not altered. The effect of a value $\lambda \neq 1$ is simply to introduce a concentration dependent diffusivity $D(C)$.

From the master curve of Fig. 8 and Eq. (4), the concentration dependence of the diffusivity can be determined for the case $\lambda = 0.2$. The result is shown in Fig. 9 where $D(C)$ can be seen to remain practically constant as the concentration is reduced to approximately one fourth of saturation, further increasing by a factor $1/\lambda = 5$ as C decreases to zero. A less abrupt transition could be obtained if a more gradual variation of $p(z)$ is assumed. It is worth pointing out that in a Fickian regime, where tensile effects are negligible compared to random motion, a concentration-dependent diffusivity may also be expected. For example in Nylon 6.6 [3], a diffusivity which increases with water concentration has been observed. The larger diffusivity at higher water concentration in the Fickian regime of this polymer, arises from an increasing concentration of ''free'' water as opposed to water more strongly bound to specific regions of the polymeric chains. In such cases, one could expect two competing effects as the water concentration increases to values where non-Fickian behavior may be approaching. The diffusivity would tend to increase with water concentration because of an exchange between ''free'' and ''bound'' water and to decrease because of tensile effects. From the arguments presented above, one would expect the occurrence of a broad maximum in the diffusivity at higher concentration, as a precursor of non-Fickian behavior.

The onset of a regime where tensile effects become important appears to be accompanied by non-Fickian transport. Profiles such as those of Fig. 3 should be observable in saturated systems with a porous structure where the breakage of connectivity has a relatively small probability. Although external conditions may play a role [4], some classes of materials are more likely to exhibit this behavior. It is expected to be observable when the solid matrix consisting of polymeric chains, shrinks as the system dries. In systems which do not behave in this manner, a gas phase can be expected to be present. The formation of minute gas bubbles during the drying process could disrupt connectivity and suppress the effect of tensile forces upon the profiles.

IV. CONCLUSIONS

A Monte Carlo algorithm for Fickian diffusion has been modified to include tensile effects. The interplay between random motion and tensile forces, which tend to preserve the integrity of clusters of diffusers, appears to be essential to explain experimental MRI profiles in a MFG. With the help of Boltzmann's transformation, the onset of a non-Fickian regime, caused by this collective motion, has been ascertained and its details explored. Although our transport model could be made more realistic, its main features should provide a valid description of water transport in saturated porous systems as revealed by MRI, with its inherent space and time scales.

ACKNOWLEDGMENTS

We wish to thank F. G. Brady Moreira, L. A. Colnago, and B. Stosic for helpful discussions. This work was supported by Conselho Nacional de Desenvolvimento Cientifico e Tecnológico and Financiadora de Estudos e Projetos (Brazilian agencies).

[1] R. J. Gummerson, C. Hall, W. D. Hoff, R. Hawkes, G. N. Holland, and W. S. Moore, Nature (London) **281**, 56 (1979).
[2] S. Blackband and P. Mansfield, J. Phys. C **19**, L49 (1986).
[3] P. Mansfield, R. Bowtell, and S. Blackband, J. Magn. Reson. **99**, 507 (1992).
[4] W. Schrader and J. B. Litchfield, Drying Technol. **10(2)**, 295 (1992).
[5] P. L. de Sousa, M. Engelsberg, M. A. Matos, and L. A. Colnago, Meas. Sci. Technol. **9**, 1982 (1998).
[6] P. T. Callaghan, A. Coy, T. P. J. Halpin, D. Mac Gowan, K. J. Packer, and F. O. Zelaya, J. Chem. Phys. **97**, 651 (1992).
[7] P. T. Callaghan and A. Coy, Phys. Rev. E **68**, 3176 (1992).
[8] S. Matsukawa and I. Ando, Macromolecules **30**, 8310 (1997).
[9] M. J. McCarthy and E. Perez (unpublished).
[10] B. Biquet and T. P. Labuza, J. Food Proc. Pres. **12**, 151 (1988).
[11] P. S. Belton, B. P. Hills, and E. R. Rimbaud, Mol. Phys. **63**, 825 (1988)).
[12] I. Mrani, G. Fras, and J. C. Benet, J. Phys. III **5**, 985 (1995).
[13] M. M. Chui, R. J. Phillips, and M. J. McCarthy, J. Colloid Interface Sci. **174**, 336 (1995).
[14] H. D. Middendorf, Physica B **226**, 113 (1996).
[15] J. Crank, *The Mathematics of Diffusion* (Oxford University Press, London, 1975), 2nd Ed.
[16] P. L. de Sousa, M. Engelsberg, and F. G. Brady Moreira, Phys. Rev. E **60**, R1174 (1999).
[17] P. G. de Gennes, J. Chem. Phys. **55**, 572 (1971).
[18] A. W. Overhauser, Phys. Rev. **92**, 411 (1953).
[19] D. J. Lurie, in *Encyclopedia of Nuclear Magnetic Resonance*, edited by D. M. Grant and R. K. Harris (Wiley, New York, 1995).
[20] M. H. Zimmerman, *Xylem Structure and the Ascent of Sap* (Springer-Verlag, Berlin, 1988) [see also, Sci. Am. **208**, 133 (1963)].
[21] S. Crestana and A. N. D. Posadas, in *Fractals in Soil Science*, edited by P. Baveye, J. Y. Parlange, and B. A. Stewart (CRC Press, Boca Raton, FL, 1998).
[22] D. Wilkinson and J. F. Willemsen, J. Phys. A **16**, 3365 (1983).